Magnetic phase diagram and anisotropy of pseudoternary $(Er_xDy_{1-x})_2Fe_{14}B$ compounds

M. R. Ibarra, P. A. Algarabel, C. Marquina, J. I. Arnaudas, and A. del Moral
Instituto de Ciencia de Materiales de Aragón and Departamento de Física de la Materia Condensada, Facultad de Ciencias, Universidad de Zaragoza, E-50009 Zaragoza, Spain and Consejo Superior de Investigaciones Científicas, E-50009 Zaragoza, Spain

L. Pareti, O. Moze, G. Marusi, and M. Solzi
Istituto di Materiali Speciali per Elettronica e Magnetismo del Consiglio Nazionale delle Ricerche, via Chiavari 18/A, I-43100 Parma, Italy
(Received 7 July 1988)

A complete study of the magnetic phase diagram and magnetic anisotropy of pseudoternary $(Er_xDy_{1-x})_2Fe_{14}B$ compounds has been carried out by the use of low-field ac magnetic susceptibility, magnetization, and singular-point detection measurements on magnetically aligned samples. A cone magnetic structure has been observed in compounds with $0.6 \leq x < 0.9$, even at low temperatures, and the thermal dependence of the cone angle for each concentration has been determined. Substitution of Er by Dy gives rise to a significant modification of the magnitude and temperature dependence of the anisotropy field H'_A (i.e., the field on the basal plane), a linear dependence being observed with Dy concentration at 293 K. The present data have been interpreted in terms of a crystalline-electric-field–mean-field model. The inclusion of only second- and fourth-order crystal-field terms is enough to account for the phase diagram and the cone magnetic structure. The fourth-order terms should necessarily be included into the Hamiltonian in order to account for the variation of angle of the cone magnetic structure, both with temperature and concentration.

I. INTRODUCTION

In addition to the outstanding permanent magnet properties of compounds based on the well characterized $Nd_2Fe_{14}B$ tetragonal crystal structure,[1–4] a great deal of interesting magnetic phenomena such as spin-reorientation transitions[3,5–7] and first-order field-induced magnetization processes (FOMP) are displayed.[8–10] It is generally accepted that such behavior can be attributed to the strong influence of the rare-earth crystalline electric field (CEF),[11–13] which increases at low temperatures. A large insight into the microscopic behavior of the magnetic anisotropy in these compounds can be obtained by investigating the nature of strong competing anisotropies arising from the R (rare-earth) sublattice. A suitable choice of R ions for such an investigation are Er and Dy, which have opposite signs of the second-order Stevens coefficients, α_J. In $Er_2Fe_{14}B$, there exists an easy-axis to easy-plane spin reorientation at $\cong 322$ K,[3] where the Fe sublattice, with axial anisotropy, overcomes the Er planar one. However, the axial Fe anisotropy is reinforced by the large Dy axial one in $Dy_2Fe_{14}B$.[14] Thus the system $(Er_xDy_{1-x})_2Fe_{14}B$ is ideal for an investigation of the strong competing anisotropies present in the tetragonal $Nd_2Fe_{14}B$ structure. The evolution of the spin-reorientation transition temperature with Er concentration could be expected to be a direct consequence of the interplay between planar and axial magnetocrystalline anisotropies. Previous investigations by Mössbauer spectroscopy[15,16] have shown that the spin-reorientation temperature decreases with increasing Dy concentration. However, some uncertainty persists in regard to the temperature interval over which the transition takes place and also the resulting final magnetic structure.

In order to clarify the influence of different competing anisotropies in such compounds, measurements of the dependence, with composition and temperature, of the magnetocrystalline anisotropy, low-field ac susceptibility and magnetization in $(Er_xDy_{1-x})_2Fe_{14}B$ compounds have been carried out. The results are reported in addition to an interpretation in terms of a CEF–mean-field model incorporating second- fourth-order terms.

II. EXPERIMENTAL TECHNIQUES

Polycrystalline samples of $(Er_xDy_{1-x})_2Fe_{14}B$ with $x = 1$, 0.9, 0.8, 0.7, 0.6, 0.5, 0.4, 0.2, and 0 were prepared by melting pure elements in an arc furnace under Ar atmosphere. The resulting buttons were subsequently heat treated at 900 °C for 7 d under vacuum. Monophasicity and homogeneity of the samples were verified by using thermomagnetic analysis (TMA). X-ray diffraction patterns showed lines and intensities consistent with those of the space group $P4_2/mnm$ of the $Nd_2Fe_{14}B$ structure.[1,2] Thermomagnetic analysis was also used to measure the Curie temperatures T_c for all the samples. The values of the spin-reorientation temperature T_{sr} for various Dy compositions were deduced from the temperature dependence of the low-field ac susceptibility. These measurements were performed using a modified mutual inductance Hartshorn bridge operating at 15 Hz. Such an apparatus measures the variation of the mutual inductance produced by the sample, which is, in turn, proportional to the real part of the magnetic susceptibility. The ap-

plied ac magnetic field was ≈ 35 mOe of peak value. To measure the magnetization, magnetically aligned magnetic samples were prepared by orienting powders in a constant magnetic field of 19 kOe. The powders were mixed with epoxy resin at $\approx 100\,^{\circ}$C where all the compositions display an easy axis. Polar plots of the magnetization parallel to the applied field (2 kOe) direction were performed on the oriented powders using both a vibrating sample magnetometer and an extraction one. By the use of such techniques, accurate and reliable information about any easy-cone direction, if present, was obtained.

The unique singular point detection (SPD) technique[17,18] has been used to measure the anisotropy field H_A in pulsed magnetic fields up to 300 kOe. In such a field it is usually possible to measure anisotropy fields up to 150 kOe with the SPD technique (Asti and Rinaldi[18]). This technique allows a fast and reliable determination to be made of H_A in both axial[18,19] and planar polycrystalline systems. The anisotropy field H_A is defined as the magnetic field which is required to saturate the sample in the hard direction along which the field is applied. In the case of uniaxial systems the anisotropy energy is given, for a determine temperature, by

$$E_k(\theta)=K_1\sin^2\theta+K_2\sin^4\theta+K_3\sin^6\theta\ , \tag{1}$$

where K_1, K_2, and K_3 are the phenomenological anisotropy energy constants. Consequently the anisotropy field in the basal plane (H'_A) and along the c axis (H''_A) are given, respectively, by

$$H'_A=(2K_1+4K_2+6K_3)/M_s\ , \tag{2a}$$

$$H''_A=2K_1/M_s\ ; \tag{2b}$$

both anisotropy fields can be accurately measured on our magnetically aligned samples by mean of the cited SPD technique. It is perhaps worthwhile to mention that the fields, defined in the above way, are not the usual *equivalent* anisotropy fields fixing the magnetization along the easy direction, but *applied* magnetic fields along the hard direction, which overcome the anisotropy torques. In this sense they are (H'_A and H''_A), just the reverse of those equivalent easy direction fields.[20]

III. RESULTS AND DISCUSSION

The Curie temperature was found to increase linearly in going from $Er_2Fe_{14}B$ to $Dy_2Fe_{14}B$ and the values are in good agreement with previously reported ones.[15] The temperature dependence of the low-field ac susceptibility for all the measured compounds is displayed in Fig. 1. There are very clear anomalies for $x>0.5$ and these are associated with a spin-reorientation process. In $Er_2Fe_{14}B$, the anomaly at 322 K is related to the spin reorientation towards the basal plane, due to the planar Er^{3+} sublattice anisotropy overcoming that of the Fe sublattice. For increasing Dy concentration, the spin-reorientation temperature decreases. The results of the measurements of the cone angle by means of the polar plots of the magnetization, parallel to the applied field, are shown in Fig. 2. It is clear that, apart from pure $Er_2Fe_{14}B$ and $(Er_{0.9}Dy_{0.1})_2Fe_{14}B$, the spin-reorientation transition is not complete, being from easy axis to easy cone, the cone angle at low temperatures decreasing with increasing Dy composition. Examples of polar plots of the magnetization are displayed in Figs. 3(a)–3(f) for $x=0.9$ and 0.8 at selected temperatures and they clearly show the relevant minima and maxima corresponding to the cone angle. The axis-to-cone transition observed here is in some contradiction with Mössbauer investigations which implied a complete axis to plane transition.[15,16] The measurements of the polar plots of the magnetization reported here enable a precise determination to be made of the cone angle.

A. Anisotropy fields

The SPD measurements have been performed on oriented powder specimens in order to enhance the signal-to-noise ratio. However, due to the high values of the anisotropy field H'_A, it was not possible to measure it

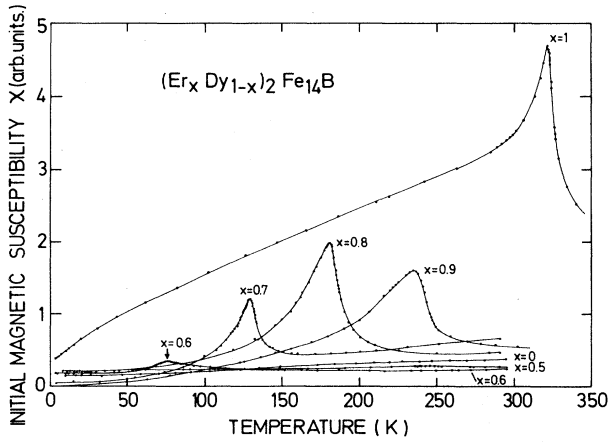

FIG. 1. Thermal dependence of ac initial magnetic susceptibility (in arbitrary units) in the pseudobinary compounds $(Er_xDy_{1-x})_2Fe_{14}B$ for different concentrations of the anisotropic R^{3+} ions.

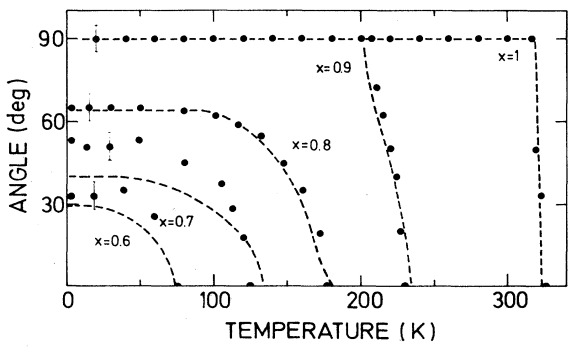

FIG. 2. Temperature dependence of the measured cone angle θ, between the c axis and the easy direction of magnetization, for $(Er_xDy_{1-x})_2Fe_{14}B$ compounds. (●), experimental results; (— — —) theoretical prediction.

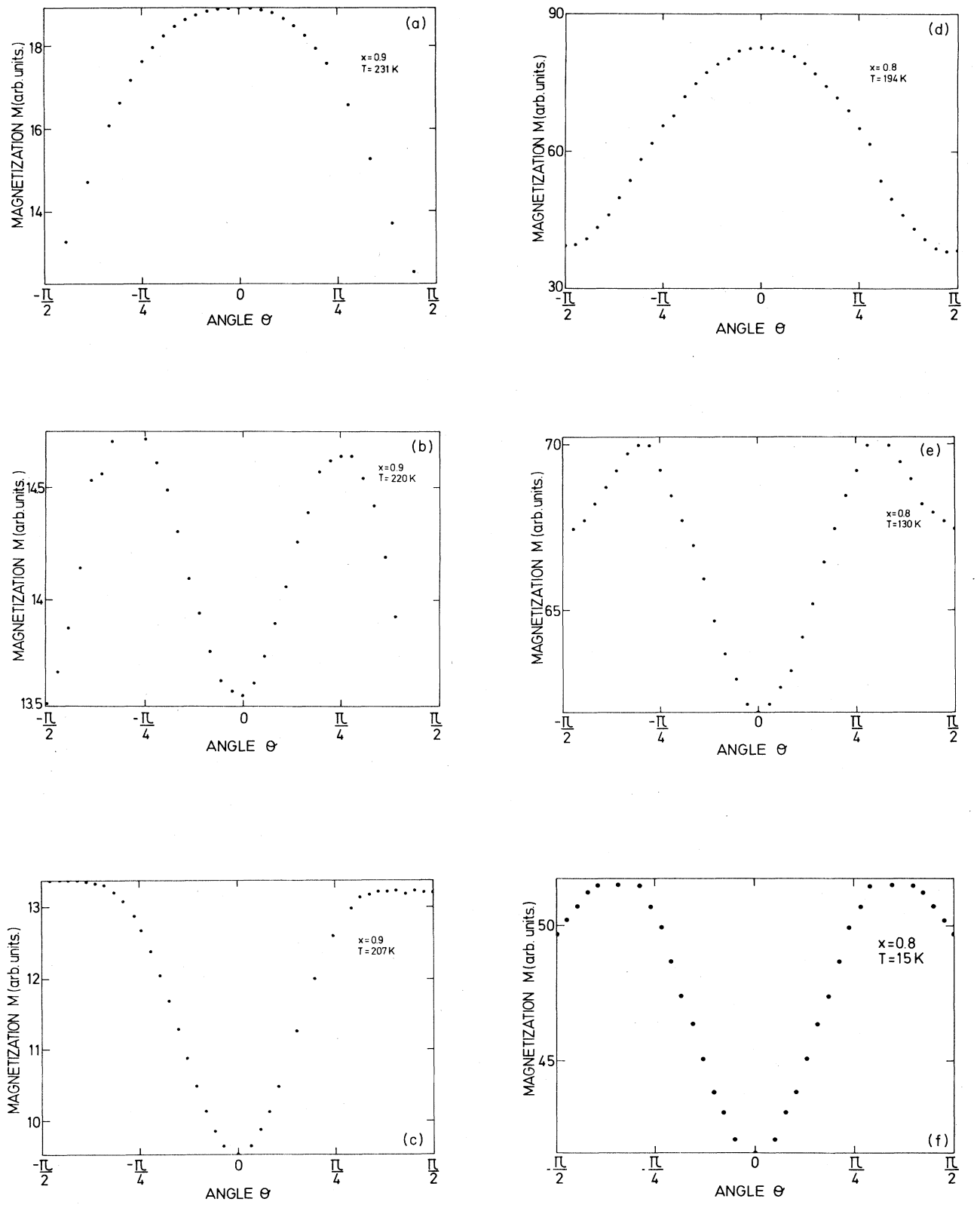

FIG. 3. Polar plots of the magnetization for $(Er_xDy_{1-x})_2Fe_{14}B$ compounds for $x=0.9$ (a), (b), and (c), and 0.8 (d), (e), and (f) for some selected temperatures. θ is the angle formed by the applied magnetic field with the tetragonal c axis.

for compositions with $x<0.5$. Dysprosium substitution has been found to greatly modify both the magnitude and the temperature dependence of the anisotropy field. The values of H'_A, measured at 293 K and reported versus Er composition x in Fig. 4, show an almost linear dependence with Dy composition, $1-x$. On the basis of an extrapolation of the present data, $Dy_2Fe_{14}B$ should have an anisotropy field larger than 290 kOe at 293 K. In Fig. 4, the calculated variation of the combination of anisotropy energy constants $K_1+2K_2+3K_3$ ($=H'_AM_s/2$) at 293 K is also reported. A linear dependence of the anisotropy constants with x would indicate that only second-order terms in the anisotropy energy expansion are important at 293 K. Thus the observed departure from a linear behavior implies the existence of non-negligible high-order anisotropy constants. The competition between Er and Dy anisotropies could account for these terms.[21] The saturation magnetization values M_s, used to calculate the sum of the anisotropy constants $K_1+2K_2+3K_3$ in pseudoternary $(Er_xDy_{1-x})_2Fe_{14}B$ compounds have been obtained by extrapolating the available data on $Er_2Fe_{14}B$ and $Dy_2Fe_{14}B$ single crystals,[3] considering a linear composition dependence of M_s. This can be done with reasonable confidence due to the localized character of the contribution of the R^{3+} ions to the total magnetic moment, i.e., $\mu=x\mu_{Er}+(1-x)\mu_{Dy}$. The temperature dependence of the anisotropy field for Dy compositions up to $x=0.5$, measured with the field applied in the basal plane, H'_A [Eq. (2a)] and along the c axis, H''_A [Eq. 2b)] are displayed in Figs. 5 and 6, respectively. For $x=0.9$, H'_A decreases with decreasing temperature (Fig. 5), reaching zero at T_{sr2}, that is the temperature value at which the system is easy plane. With increasing Dy content, the temperature dependence of H'_A is reversed (H'_A increases with decreasing temperature for $x<0.9$)

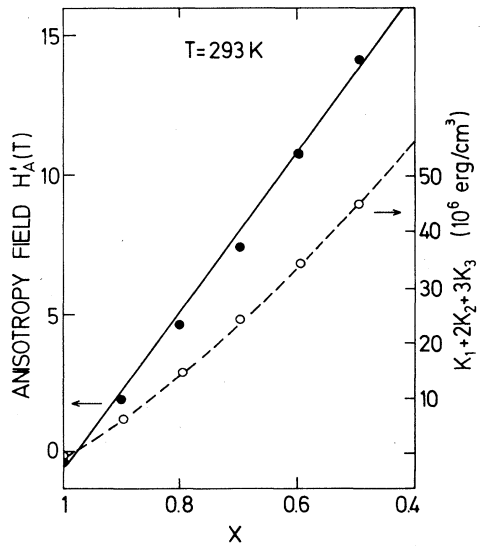

FIG. 4. Compositional dependence of the measured anisotropy field H'_A and the calculated combination of anisotropy energy constants $K_1+2K_2+3K_3$ at 293 K for $(Er_xDy_{1-x})_2Fe_{14}B$ compounds.

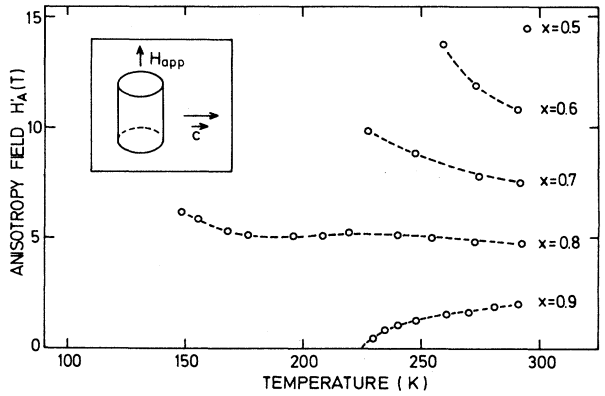

FIG. 5. Temperature dependence of the anisotropy field H'_A for magnetically aligned powders of $(Er_xDy_{1-x})_2Fe_{14}B$ compounds. The field is applied perpendicular to the direction of alignment, which at 373 K is the c axis.

and the slope is enhanced. Considering that $(Er_xDy_{1-x})_2Fe_{14}B$ compounds with $x>0.5$ display a spin-reorientation transition (K_1 changes sign) with decreasing temperature, the observed variation of H'_A for $x\leq 0.8$ implies that at low temperatures, high-order positive anisotropy constants become dominant with increasing Dy concentration.

The temperature dependence of the anisotropy field is altered by addition of Dy also in the hard c-axis region. An enhancement in the slope of the H''_A versus temperature curve is, in fact, observed with increasing Dy content. It should be emphasized that H''_A reaches a value of zero at T_{sr1}, i.e., the temperature at which the magnetization vector starts to tilt away from the c axis (K_1 changes sign). The calculated values of $K_1+2K_2+3K_3$ in the hard-plane region and K_1 in the hard-axis region are reported versus temperature for $(Er_xDy_{1-x})_2Fe_{14}B$ in Fig. 7. The temperature dependence of the anisotropy constants confirms the conclusions, obtained from the magnetization measurements, concerning the final state of the system after the spin-reorientation transition. It is partic-

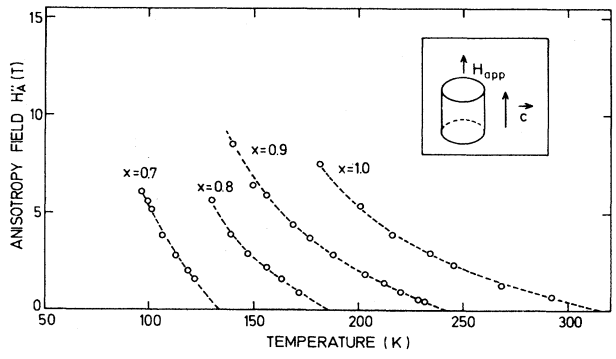

FIG. 6. Temperature dependence of the anisotropy field H''_A for magnetically aligned powders of $(Er_xDy_{1-x})_2Fe_{14}B$ compounds. The field is applied parallel to the direction of alignment, which at 373 K is the c axis.

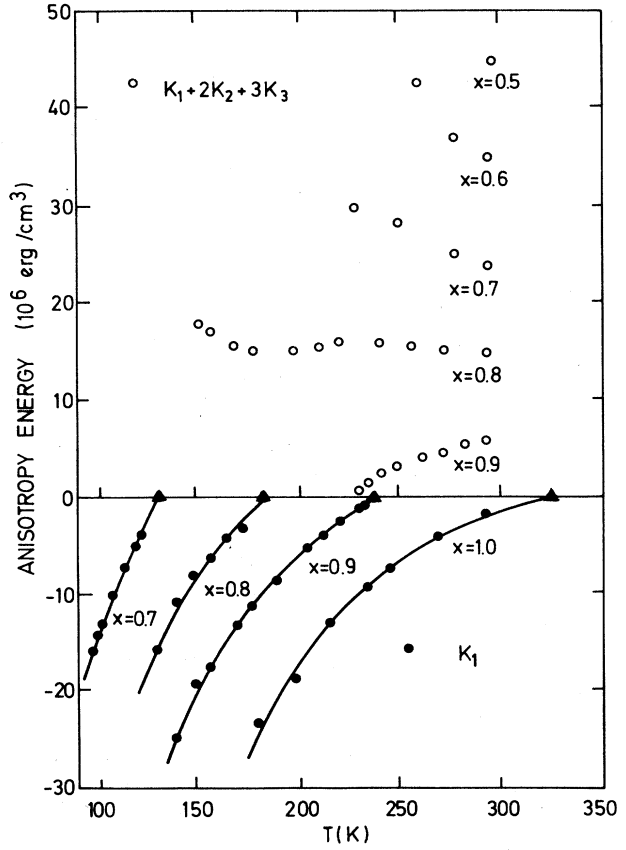

FIG. 7. Calculated values of the anisotropy energy constants $K_1+2K_2+3K_3$ and K_1 for $(Er_xDy_{1-x})_2Fe_{14}B$ compounds. (0) $K_1+2K_2+3K_3$; (●) K_1; (▲) obtained from ac initial magnetic susceptibility measurements.

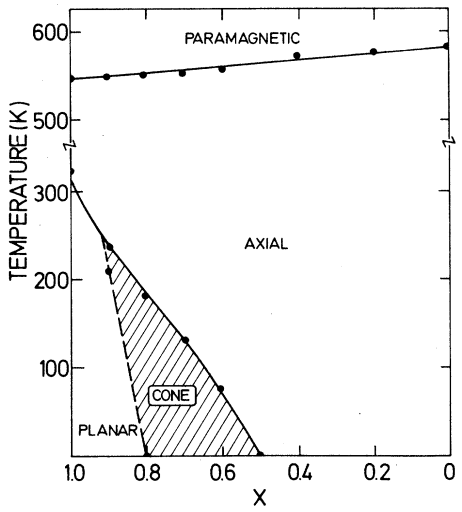

FIG. 8. The magnetic phase diagram for the series of $(Er_xDy_{1-x})_2Fe_{14}B$ compounds.

ularly clear that for $x=0.9$, a temperature T_{sr1} (where $K_1=0$, i.e., the reorientation starts and M_s tilts away from the c axis) and a temperature T_{sr2} (where $K_1+2K_2+3K_3=0$, which means that the system has reached an easy-plane configuration), can be obtained. Whilst a T_{sr1} can be defined for compounds with $x=0.7$ and 0.8 ($K_1=0$), no T_{sr2} can be defined, as the spin reorientation takes place from easy axis to easy cone. The complete magnetic phase diagram incorporating the results of the low-field susceptibility, magnetization and SPD measurements is displayed in Fig. 8.

B. Spin reorientation and CEF model

In order to account for the observed behavior in the spin-reorientation region of the pseudoternary $(Er_xDy_{1-x})_2Fe_{14}B$ compounds, a single-ion CEF model has been used to describe the contributions from the Er^{3+} and Dy^{3+} ions to the anisotropy energy. A two-dimensional molecular-field approximation has been used for the exchange interaction, where the exchange field coupling the R^{3+} ion and the Fe sublattice is confined to the x-z place (z corresponds to the c axis [001] and x to the [100] direction) in order to avoid the imaginary component of the total R^{3+} angular momentum. The free energy is calculated for every position of the magnetic moment in the plane[15,22] making an angle θ with the c axis.[15,22] The anisotropy energy contribution from the Fe sublattice is also included in the total free energy. An important assumption in the present method is to consider that the exchange coupling stabilizes collinearity between the effective magnetic moments of the Fe sublattice and of the R one, being ferromagnetic for light R and ferrimagnetic for heavy R ions.

The CEF Hamiltonian appropriate for the different R ions (Er^{3+} and Dy^{3+}) having mm point symmetry has been considered up to fourth order, in the form

$$H^R_{\rm CEF}=B^0_2O^0_2+B^2_2O^2_2+B^0_4O^0_4\ , \tag{3}$$

where $R=$Er and Dy and where B^m_n and O^m_n are the CEF parameters and Stevens operators, respectively. Remember that both Dy^{3+} and Er^{3+} ions have the same $J=\frac{15}{2}$, although we have to distinguish between different CEF parameters. The exchange Hamiltonian is given by

$$\begin{aligned} H^R_{\rm ex}&=-g_J\mu_B\mathbf{H}_{\rm mol}\cdot\mathbf{J}\\ &=-2(g_J-1)\mu_B\mathbf{J}\cdot\mathbf{H}_{\rm ex}\\ &=-g_J\mu_BH_{\rm mol}(J_z\cos\theta+J_x\sin\theta)\ , \end{aligned} \tag{4}$$

TABLE I. Crystal-field (CEF) parameters (in K) obtained from the fit of the thermal dependence of the cone angle for several concentrations of the series $(Er_xDy_{1-x})_2Fe_{14}B$.

	B^0_2	B^2_2	B^0_4
$Er^{3+}(4f)$	+0.35±0.05	±0.10±0.05	−(8±0.5)×10^{-4}
$Er^{3+}(4g)$	+0.33±0.05	±0.30±0.15	−(8±0.5)×10^{-4}
$Dy^{3+}(4f)$	−1.37±0.01	+0.285±0.005	+(5±1)×10^{-3}
$Dy^{3+}(4g)$	−1.27±0.01	+0.85±0.01	+(5±1)×10^{-3}

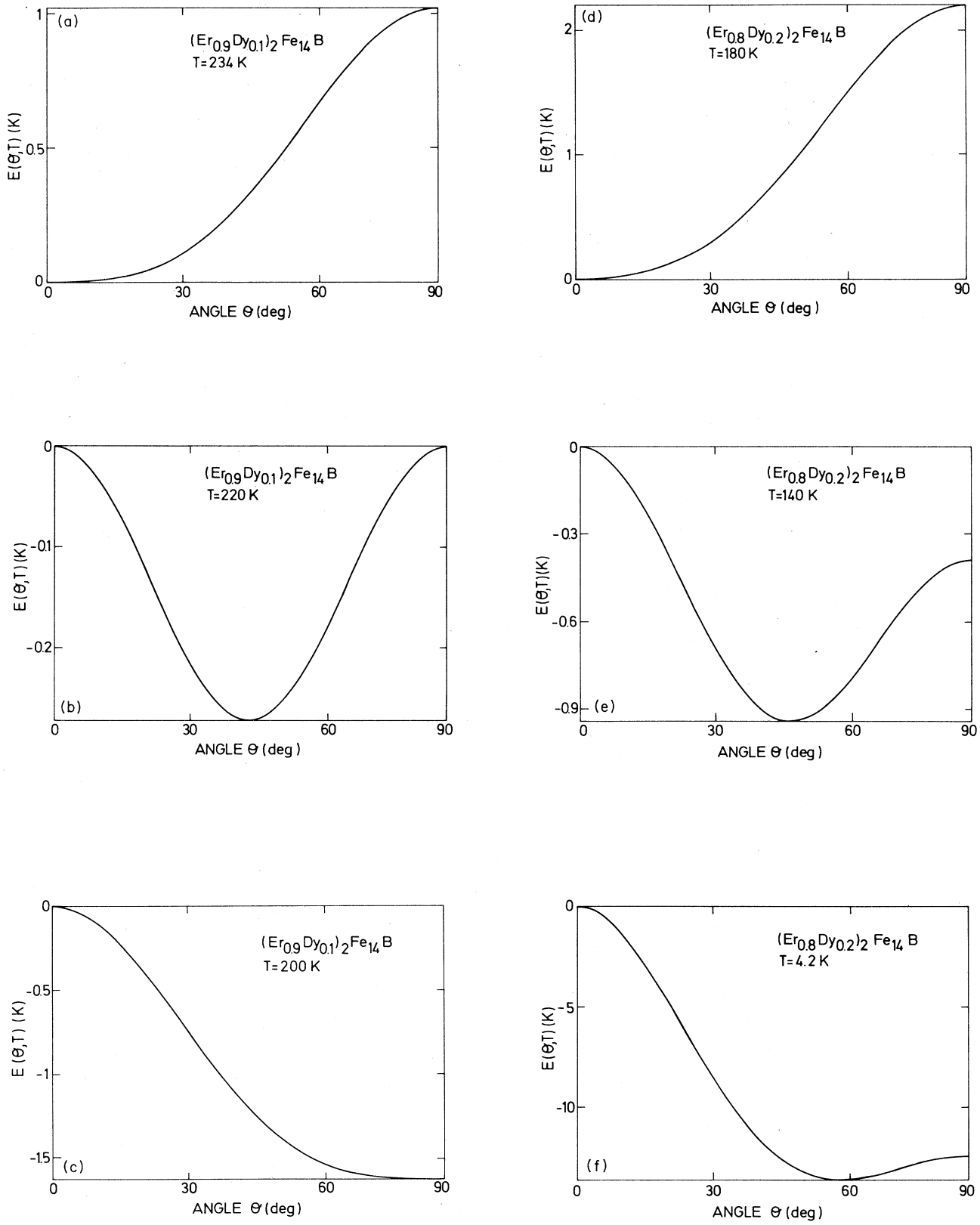

FIG. 9. Calculated values of the total free energy $F(\theta, T)$ for $(Er_xDy_{1-x})_2Fe_{14}B$ compounds for $x=0.9$ (a), (b), and (c) and 0.8 (d), (e), and (f), at selected temperatures. The minima signal the easy direction of magnetization.

where R =Er, Dy, and H_{mol} is the molecular field arising from the Fe sublattice and is related to the exchange field by $H_{mol}=[2(g_J-1)/g_J]H_{ex}$. H_{ex} is the exchange field describing the spin angular momentum $4f$-$3d$ exchange which can be considered constant for a series of compounds which are isostructural. The values used for the molecular field were obtained from Ref. 15 and refined further in the fitting process [$H_{mol}(Er^{3+})=62$ K$/g_J\mu_B$ and $H_{mol}(Dy^{3+})=94$ K$/g_J\mu_B$] and the usual temperature dependence for $H_{mol}(T)$ was also employed, i.e.,

$$H_{mol}(T)=H_{mol}(0)\left[1-0.5\left[\frac{T}{T_0}\right]^2\right] . \quad (5)$$

The operators J_z, J_x are those associated with the components of the R^{3+} angular momentum. The free energy is obtained by diagonalization of the total Hamiltonian $H=H_{CEF}+H_{ex}$ within the ground-state manifold J and then calculating the partition function $Z(\theta,T)$. The free energy is

$$F(\theta,T)=-K_BT\ln Z(\theta,T) . \quad (6)$$

The free energy per R^{3+} ion can be written as

$$F_R(\theta,T)=xF_{Er}(\theta,T)+(1-x)F_{Dy}(\theta,T) , \quad (7)$$

where we have assumed that Er^{3+} and Dy^{3+} are randomly distributed over the two $4f$ and $4g$ sites that the R^{3+} ions occupy in this crystalline structure. A further assumption has been made in order to obtain the values of the CEF parameters for the individual $4f$ and $4g$ sites (see Table I). This assumption considers the relationships which exist between the individual and arithmetic average CEF second-order parameters,[15] B_2^0 and B_2^2, in order to obtain those individual values from our forcibly averages ones obtained in the way explained below. For that we have taken into account the electric field gradient (EFG) parameters for the two Gd sites in $Gd_2Fe_{14}B$ (Ref. 23) in the way already used by Rechenberg *et al.*[15] The total energy for the system $F(\theta,T)=F_R(\theta,T)+F_{Fe}(\theta,T)$ has been obtained by considering the contribution from the Fe sublattice per R ion as

$$F_{Fe}(\theta,T)=K_1(T)\sin^2\theta . \quad (8)$$

The temperature dependence of $K_1(T)$ was obtained from anisotropy measurements on $Y_2Fe_{14}B$.[24] The angular dependence of the total free energy was then evaluated and the minimum in the free energy shall give the orientation of the total magnetization vector. The calculated free energies as a function of θ, for $x=0.9$ and 0.8, are displayed in Fig. 9 for some selected temperatures, in the easy axis-easy plane and easy axis-easy cone transition regions for the two compounds, respectively. The calculated values of the temperature dependence of the cone angle θ for $x\geq 0.6$ are displayed in Fig. 2 together with the experimentally observed values. Indeed this fitting procedure allows us to determine average (among the random occupation $4f$ and $4g$ sites) values of B_2^0, B_2^2, and B_4^0, although distinguishing between both R^{3+} species. The agreement is really quite good at high Er^{3+} concentrations ($x=0.8$, 0.9, 1) and it constitutes a confirmation that CEF terms of only up to fourth order are enough to account for the observed cone magnetic structure in $(Er_xDy_{1-x})_2Fe_{14}B$ compounds. Nevertheless some discrepancy has been observed for $x=0.6$ and 0.7 although is not possible to exactly explain the thermal dependence of the coning angle, however, we can predict the temperature at which the spin-reorientation transition starts.

The use of only second-order terms to describe the CEF interaction allows us to explain the experimental phase diagram obtained for this series (see Fig. 8), in the sense that we can predict the existence of an intermediate magnetic cone structure for concentrations below $x=0.8$, in good agreement with the recent results obtained by Boltich *et al.*[25] But nevertheless, it is not possible by using only second-order terms, to explain neither the existence of the spin reorientation for the concentration $x=0.6$ nor to fit the experimental values obtained for the cone angle of the easy magnetization direction as a function of temperature for several concentrations. It was necessary, however, to introduce fourth-order terms B_4^0 in the CEF Hamiltonian. From our point of view, the values that we have determined for the site CEF parameters for the Er^{3+} and Dy^{3+} ions in these systems, as mentioned before (see values on Table I), are rather accurate, and in fact they are not far from the values given in Refs. 15 and 24. However, the refining process that we have performed fitting the cone angle for each concentration as a function of the temperature, constitutes a very strict test of our CEF model and also the reliability of the determined CEF parameters.

[1]J. F. Herbst, J. J. Croat, F. E. Pinkerton, and W. B. Yelon, Phys. Rev. B **29**, 4176 (1984).
[2]C. B. Shoemaker, D. P. Shoemaker, and R. Fruchart, Acta Crystallogr. C **40**, 1665 (1984).
[3]S. Hirosawa, Y. Matsuura, H. Yamamoto, S. Fujimara, M. Sagawa, and H. Yamauchi, J. Appl. Phys. **59(3)**, 873 (1986).
[4]K. H. J. Buschow, Mater. Sci. Rep. **1**, 1 (1986).
[5]D. Givord, H. S. Li, and R. Perrier de la Bathie, Solid State Commun. **51**, 857 (1984).
[6]R. L. Davis, R. K. Day, and J. B. Dunlop, Solid State Commun. **56**, 181 (1985).
[7]R. Fruchart, P. L'Heritier, P. Dalmas de Reotier, D. Fruchart, P. Wolfers, J. M. D. Coey, L. P. Ferreira, R. Guillen, P. Vulliet, and A. Yaouanc, J. Phys. F **17**, 483 (1986).
[8]G. Asti and F. Bolzoni, J. Magn. Magn. Mater. **20**, 29 (1980).
[9]L. Pareti, F. Bolzoni, and O. Moze, Phys. Rev. B **32**, 7604 (1985).
[10]F. Bolzoni, O. Moze, and L. Pareti, J. Appl. Phys. **62**, 615 (1988).
[11]J. M. D. Coey, J. Less Common Met. **126**, 21 (1986).
[12]J. M. Cadogan and J. M. D. Coey, Phys. Rev. B **30**, 7326 (1984).
[13]E. B. Boltich and W. E. Wallace, Solid State Commun. **55**, 529 (1985).

[14]H. Hiroyoshi, N. Saito, G. Kido, Y. Nakagawa, S. Hirosawa, and M. Sagawa, J. Magn. Magn. Mater. **54-57**, 583 (1986).
[15]H. R. Rechenberg, J. P. Sanchez, P. L'Heritier, and R. Fruchart, Phys. Rev. B **36**, 1865 (1987).
[16]D. Niarchos and A. Simopoulos, Solid State Commun. **59**, 669 (1986).
[17]G. Asti and S. Rinaldi, J. Appl. Phys. **45**, 3600 (1974).
[18]G. Asti and S. Rinaldi, Phys. Rev. Lett. **28**, 1584 (1972).
[19]F. Bolzoni, F. Leccabue, and L. Pareti, Appl. Phys. Lett. **7**, 37 (1980).
[20]F. Brailsford, *Physical Principles of Magnetism* (Van Nostrand, London, 1966), p. 124.
[21]S. Rinaldi and L. Pareti, J. Appl. Phys. **50(11)**, 2219 (1979).
[22]M. R. Ibarra, E. W. Lee, A. del Moral, and O. Moze, Solid State Commun. **53**, 183 (1985).
[23]M. Boge, G. Czjzek, D. Givord, C. Jeandey, H. S. Li, and J. L. Oddon, J. Phys. F **16**, L67 (1986).
[24]F. Bolzoni, J. P. Gavigan, D. Givord, H. S. Li, O. Moze, and L. Pareti, J. Magn. Magn. Mater. **66**, 158 (1987).
[25]E. B. Boltich, F. Pourarian, R. T. Obermayer, S. G. Sankar, and E. W. Wallace, J. Appl. Phys. **63**, 3964 (1988).